

A new approach to exploring architecture of bipartite (interaction) ecological networks

JÁNOS PODANI[†]

Department of Plant Systematics, Ecology and Theoretical Biology, Institute of Biology, L. Eötvös University, Pázmány P. s. 1/C, H-1117 Budapest, Hungary and Ecology Research Group of the Hungarian Academy of Sciences, Pázmány P. s. 1/C, H-1117 Budapest, Hungary

[†]Corresponding author: podani@ludens.elte.hu

FERENC JORDÁN

The Microsoft Research, University of Trento Centre for Computational and Systems Biology (COSBI), Piazza Manifattura 1, 38068 Rovereto (TN), Italy and Balaton Limnological Institute, Centre for Ecological Research, Hungarian Academy of Sciences, Klebelsberg K. u. 3, H-8237 Tihany, Hungary

AND

DÉNES SCHMERA

Section of Conservation Biology, University of Basel, St. Johannis-Vorstadt 10, CH-4056 Basel, Switzerland and Balaton Limnological Institute, Centre for Ecological Research, Hungarian Academy of Sciences, Klebelsberg K. u. 3, H-8237 Tihany, Hungary

Edited by: Ernesto Estrada

[Received on 17 November 2013; accepted on 9 January 2014]

We propose the use of a new methodological scheme for exploring and quantifying structure in bipartite ecological networks. In this, graphical visualization and numerical measurement are combined, offering a unique possibility for network analysis on a coherent conceptual basis. Dissimilarity between all species pairs in either group of constituting species, calculated based on their interactions with the other group, is decomposed into additive fractions expressing link replacement and degree difference of nodes. Together with interaction similarity, these are used to visualize network features in form of a two-dimensional simplex diagram. Furthermore, these quantities serve as a basis for characterizing and measuring nestedness, architectural asymmetry as well as bimodality in the distribution of interaction dissimilarity, which in turn can be used to detect modularity in the graph. The approach is extended to weighted links, facilitating comparisons with the unweighted version of the same network, which was an old but unresolved issue in network science. This is especially important for nestedness and modularity whose measurement has been confined mostly to unweighted networks. The use of the method is demonstrated by artificial graphs and on selected examples of actual ecological network data. We suggest that the methods apply equally well to bipartite graphs used in other fields of science as well.

Keywords: asymmetry; connectance; Jaccard dissimilarity; modularity; nestedness; simplex.

1. Introduction

Interactions between two groups of species from the same assemblage have been routinely summarized in ecology by bipartite networks [1–6]. In graph theoretical terms, a bipartite network consists of two sets of vertices or nodes corresponding to two kinds of species and a collection of edges or links, such that no vertices from the same set are adjacent [7]. These relations most commonly include host–parasite, plant–seed disperser, plant–pollinator and plant–herbivore interactions, although other types (plant–ant, anemone–fish, mycorrhiza–plant) have also been studied intensively. The reasons for the steadily growing interest in these graphs are obvious because, for example, knowledge of host–parasitoid networks may provide useful solutions for biological control [2], whereas plant–pollinator networks may help us to manage the current pollination crisis [1]. It is also of primary theoretical importance to show whether these biological types of networks are different in basic architectural features, such as nestedness and modularity, and if so, to reveal the ecological background behind the differences.

Large amounts of data have been available for studying ecological bipartite graphs (see databases offered by Jordano [8] and NCEAS [9]), and a wide variety of visualization and analytical tools have been developed and applied to them [10–14]. Although graphs themselves are conceived generally as the most appropriate tools to summarize and visualize relations between sets, simple graphical displays usually fail to provide comprehensible views for a large number of nodes and complex systems of links. The ecological literature abounds in illustrations of bipartite networks which are impossible to interpret by the naked eye. Thus, visualizing the detailed structure of a large interaction network is often a challenge and serves more like an art than to facilitate understanding. A mathematically equivalent summarization of a bipartite network is the adjacency (or interaction) matrix with one set of species in rows and the other set as columns. An entry in this matrix is 1 if the two species in question are related, and 0 otherwise. The structure of the matrix and the corresponding graph may be obvious by looking at the two-dimensional arrangement of 1's and 0's, but successful visual interpretation always depends on the order of rows and columns. If ordering is optimized for one feature of the graph (e.g. nestedness); the same arrangement may be much less informative for another (e.g. modularity, see Figs 2 and 3 in [12] or Fig. 2 in [15]). Thus, matrix representations may also perform poorly and therefore insufficient by themselves for depicting network architecture appropriately. Simultaneous ordination of rows and columns of the adjacency matrix by correspondence analysis (CA) may be a promising approach to revealing network structure, as demonstrated in [12] using artificial interaction matrices. For actual data, however, CA has only been used to find a one-dimensional ordering of species, thus focusing on the diagonal structure of the interaction matrix. Further aid in interpreting graph structure is offered by dozens of various coefficients expressing a particular property of the graph in terms of a single coefficient value. The precise relationships between these properties are not yet known sufficiently, which may slow down predictability and applicability. Although there have been several studies reporting on comparisons of these functions and discussing their relative merits (see especially [14]), the interpretation of coefficient values is not always straightforward. Moreover, many of them (e.g. the clustering coefficient) apply only to food webs and are less interpretable for bipartite networks. We are convinced that a new framework may be useful which *combines graphical visualization with numerical measurement into a single method* suited specifically to bipartite graphs, thus revealing and measuring several aspects of network structure simultaneously and efficiently.

We suggest that both the quantitative evaluation and the visualization of bipartite ecological networks could profit from the adaptation of a methodology recently developed by ourselves for matrix analysis [16,17]. The essence of the new method is the comparison of all possible pairs of species in either domain, based on the relationships to the species of the other domain as attributes, and

the decomposition of the resulting similarities and complementary dissimilarities into three additive components. These components have direct graph theoretical and ecological meaning, and can be graphically displayed by two-dimensional simplices or ternary plots for all pairs of species. Within this plot, three possibilities are available to reduce point scatter into one-dimensional simplex diagrams, each reflecting further important properties of the graph. The arrangement of points together with numerical results provides a sophisticated yet fairly easy-to-use tool for network analysis and facilitates comparisons between different situations. In agreement with the attribute duality principle, a graph (and the corresponding matrix) can and should be viewed and analysed from two perspectives: via species in the columns or via species in the rows. This leads to defining a novel measure of architectural asymmetry in bipartite networks. The distribution of pairwise dissimilarities offers a relatively simple method for evaluating modular structure as well. Further advantage of the new methodology is that it can be readily extended to weighted bipartite graphs in which interaction strength between related species is also expressed, thus allowing comparisons between unweighted and weighted representations for the same set of study objects (see also [18]). We illustrate these issues by using several toy matrices and actual ecological network data.

2. The simplex approach to bipartite networks

In this section, we place the simplex approach suggested by Podani and Schmera [16] into the context of graph analysis. While some repetitions are unavoidable, we emphasize that different components of the simplex bear new meaning when adopted to bipartite graphs. In what follows, therefore, complete description of the underlying terminology and the functions is provided.

Ecological studies of mutualistic or antagonistic relationships between organisms are concerned with two sets of partner species, P and M , containing p and m species, respectively. The bipartite network \mathbf{G} for these $p + m$ species corresponds to the interaction matrix \mathbf{X} with p rows and m columns, such that $x_{hj} = 1$ if interaction exists between species h from P and species j from the partner set M , and $x_{hj} = 0$ otherwise. For simplicity without losing generality, in this section we shall refer to the species in rows as plants (corresponding to hosts or anemones in certain network types) and to the species in columns as pollinators (here: insects, corresponding to parasites, ants, fish, herbivores and fungi in some other network types). Similarity between two pollinators j and k reflecting their relative agreement in the identity and number of plant species pollinated can be expressed by the Jaccard index [19]

$$S_{jk} = a/(a + b + c), \quad (1)$$

in which a is the number of species pollinated by both species, b is the number of species that are pollinated only by insect j and c is the number of species pollinated only by insect k . For simplicity, let $n = a + b + c$, which in turn equals $\sum_i \max(x_{ij}, x_{ik})$, while $a + b = \sum_i x_{ij}$, etc. $S_{jk} = 0$ if the two insect species pollinate completely different species, whereas $S_{jk} = 1$ if the two species pollinate the same set of plant species. Coefficient (1) is not new in network science; it has long been used to express *interaction* (trophic) *similarity* between species in food webs [20–23] and more recently in plant–pollinator networks as well [10,24].

The complement of S_{jk} is Jaccard dissimilarity

$$I_{jk} = (b + c)/n = 1 - S_{jk}, \quad (2)$$

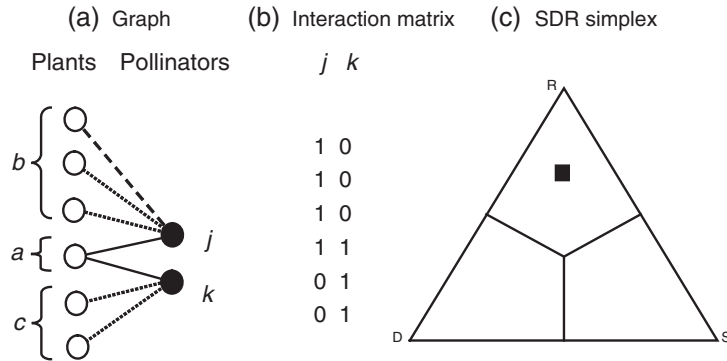


FIG. 1. Interpretation of component terms in the comparison of pollinator species j and k from a small artificial bipartite network (a) and its matrix equivalent (b). $a = 1$ is the number of plants shared (connected by solid links to both pollinators), $b = 3$ is the number of plants linked only to j , $c = 2$ is the number of plants linked only to k . $|b - c| = 1$ is the absolute degree difference between j and k (corresponding to the dashed link), while $2 \min\{b, c\} = 4$ is absolute link replacement (four dotted links). Quantities a , $|b - c|$ and $2 \min\{b, c\}$ divided by $n = a + b + c$ provide relativized measures used to determine the position of this pair in the SDR simplex (c). As seen, structure for this small graph is dominated by link replacement, while interaction similarity and degree difference have much less albeit equal significance.

which may be termed the *interaction dissimilarity* in the present context. The key issue here is that, analogously to the decomposition of Jaccard dissimilarity in case of species \times localities data matrices [16,25], interaction dissimilarity is additively divided into two fractions. The first one expresses how much the degrees of (number of links adjacent to) nodes j and k differ, and is given by

$$D_{jk} = |b - c|/n, \quad (3)$$

which is termed here the (relative) *degree difference* between the two nodes. This reflects the difference between species on a specialist-generalist continuum (i.e. the richness of their connectedness in network terms). The other fraction of dissimilarity I_{jk} is

$$R_{jk} = 2 \min\{b, c\}/n, \quad (4)$$

which expresses the proportion of the number of plants linked only to pollinator j replaced by different plant species for pollinator k , and is called the relative *link replacement* function. The meaning of a , b , c , $|b - c|$ and $2 \min\{b, c\}$ is illustrated in Fig. 1(a and b) for a small artificial example.

The basis of the present approach is the immediate observation that for any pair of pollinators $1 \leq j \neq k \leq m$, we have that $S_{jk} + D_{jk} + R_{jk} = 1$. This offers the opportunity to use a two-dimensional simplex frequently used in the natural sciences (e.g. geology) to express the relationship between three quantities with a total of 1.0. The graphical illustration of the two-dimensional simplex is an equilateral triangle, the so-called *ternary* or *simplex* plot. Here, we use the term *SDR-simplex* in which we preserve as a convention the original set-up [16], so that the lower right corner is S , the lower left is D and the top is R . In this diagram, the distance of a point (representing a pair of nodes in the graph) from a given corner is inversely proportional to the respective fraction. For instance, the point is in the centroid of the triangle if $S_{jk} = D_{jk} = R_{jk} = 1/3$. For the pollinators in the small graph of Fig. 1(a), the scores are $S_{jk} = 1/6$, $D_{jk} = 1/6$ and $R_{jk} = 4/6$ which place this pair into the upper third of the triangle (Fig. 1c). Then, if these functions are applied to all the possible pairs of pollinators, we shall have a *diagram in*

which point pattern depicts network architecture in terms of interaction similarity, relativized degree difference and relativized link replacement (Fig. 2).

The SDR-simplex may be reduced to three one-dimensional simplices by combining two values at a time and using the third one as a contrast. These are derived by perpendicular projection of points to each of the three medians of the triangle. For interaction networks, these one-dimensional simplices show trends from

- (1) Complete interaction similarity towards increasing dissimilarity: $S_{jk} = a/n$ versus $I_{jk} = D_{jk} + R_{jk} = (b + c)/n$ (*interaction dissimilarity* or *I-simplex*). The closer a pair of insects is to the *S corner*, the more similar they are in pollination behaviour. If all pollinators are connected to all plants, the network will be a complete bipartite graph and all points will lie on the corner ($S = 100\%$). Closeness to the opposing *I side* of the triangle implies high interaction dissimilarity of pollinator pairs. If the network is disintegrated into m isolated subgraphs, i.e. no pollinator shares any plant with another pollinator, then all points will lie on the left side ($I = 100\%$, Fig. 2c).
- (2) Degree difference towards increasing agreement: $D_{jk} = |b - c|/n$ versus $A_{jk} = S_{jk} + R_{jk} = (a + 2 \min\{b, c\})/n = (n - |b - c|)/n$ (*degree agreement* or *A-simplex*). If a pair of pollinators falls close to the *D corner*, it means that they have large differences in the number of associated plant species. A pair falls right onto the *D corner* ($D = 100\%$) only if one of them has no links at all, but normally no such species are included in interaction graphs. Closeness to the opposing *A side* of the triangle reflects great similarity in degree. The network is half-regular if the degree distribution with respect to the pollinators is even, i.e. all points are on the right side of the triangle ($A = 100\%$, Fig. 2c).
- (3) Link replacement towards increasing nestedness: $R_{jk} = 2 \min\{b, c\}/n$ versus $N_{jk} = S_{jk} + D_{jk} = (a + |b - c|)/n$ (*nestedness* or *N-simplex*). On this, we see the antagonistic relationship between species replacement and nestedness. A point representing a pair of pollinators falls onto the *R corner* if they share no plants and their degree is the same ($R = 100\%$). In accordance with the general view in network science [26], pairwise nestedness is understood here as a relationship between two species such that plants pollinated by either one is a subset of plants pollinated by the other. Thus, projection to the *N-simplex* is conditioned upon having at least one shared species ($a > 0$). In the *broad* sense, nestedness may be positive for pollinators even if they have the same degree (N , [16,27]), i.e. when $b = c$. However, if nestedness is restricted to pairs of pollinators that have unequal degree in the graph (as advocated by Ulrich and Almeida-Neto [28]) we speak of *strict nestedness* (N'), for which the conditions are $a > 0$ and $b \neq c$. That is, points on the left side (when $a = 0$), or on the left or the right sides of the triangle (when $a = 0$ or $b = c$), are excluded from projection to the median, respectively, when calculating N and N' . All points falling onto the *N* (bottom) side of the triangle indicate perfect nestedness of pollinators ($N = 100\%$, Fig. 2c).

For brevity, these one-dimensional simplices were named after the combined measure (Fig. 2). In addition to the graphical display, results may also be expressed numerically to enhance interpretation and comparison of different networks. The numerical output includes the mean values of S , D , R , I , A and N , the first three defining the centroid of the points within the triangle. If multiplied by 100, these quantities can be interpreted as percentage contributions to the scatter of points within the simplex (as already explained in numbered paragraphs 1–3 above). Equations are presented in Supplementary

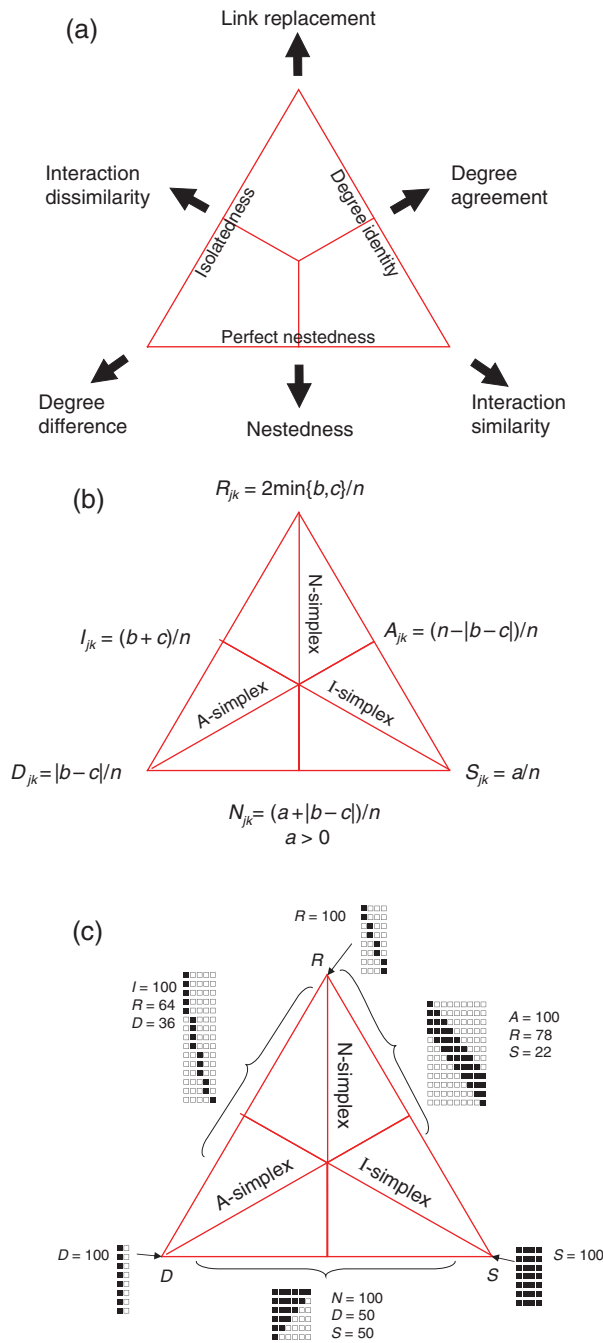


FIG. 2. The SDR simplex for bipartite networks: concepts (a), measurement (b) and small interaction matrices corresponding to extreme situations with all pairs of species (in columns) on a corner or a side (c). Full squares: presence of link, empty squares: absence; a convention followed in most figures in this paper.

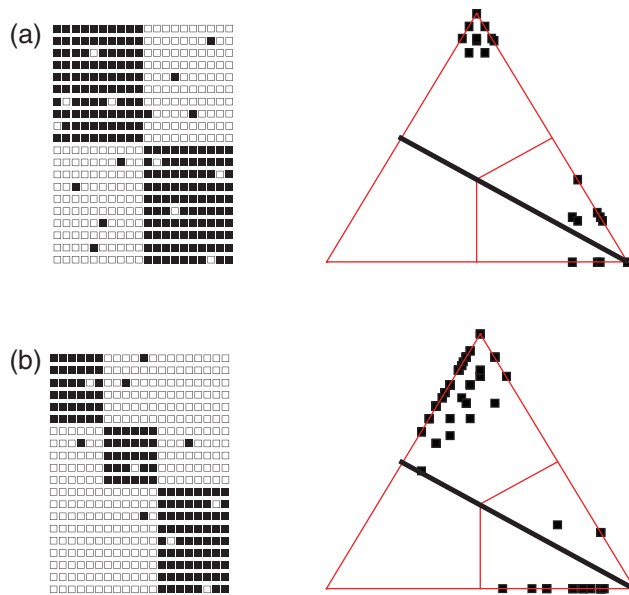


FIG. 3. The SDR simplex for strongly modular network structures, showing bimodal distribution of points (representing pairs of columns in the interaction matrices) if they are projected onto the 1-simplex (thick line).

Appendix 1. In order to get even more meaningful information on graph structure, the entire procedure described above is applied to the rows (in this case, plants) of the interaction matrix, so that *every bipartite graph is characterized by two SDR simplex diagrams and the two sets of associated percentage values simultaneously*. Thus, comparison of column-wise and row-wise analyses for $(m^2 - m)/2$ and $(p^2 - p)/2$ points, respectively, may provide insight into network architecture deeper than when structure is examined from either aspect only. Examples for two small artificial graphs and random data with three different levels of connectedness are provided in Supplementary Appendix 2, Figs A.2.1–2.

The analysis of *weighted* networks is straightforward on similar grounds. The Jaccard similarity index and its dissimilarity version have well-known counterparts for quantitative data: the Ruzicka index and the Marczewski–Steinhaus coefficient, respectively [17]. In this case, zeros in the interaction matrix reflect absence of links, while positive values indicate interaction strength between the corresponding species pair (e.g. frequency of visits on flowers, prevalence). In other words, each 1 in matrix \mathbf{X} is replaced by a positive weight value. All functions described above have their weighted variants, distinguished in this text by an upper index ‘ w ’ preceding each symbol (${}^wS_{jk}$, ${}^wN_{jk}$, etc.). Details of calculation are described in Supplementary Appendix 1; an example is presented in Supplementary Appendix 2, Fig. A.2.3. However, in the forthcoming discussion, a network is understood as an unweighted one, unless otherwise specified.

3. Detection of modular structures based on simplex scores

The SDR simplex directly expresses many aspects of network architecture simultaneously, but it is not yet shown whether *modularity*, another frequently examined property of ecological bipartite networks, can also be assessed this manner. The term module has been defined in a wide variety of ways in the ecological literature. Modules are sometimes understood as ‘any identifiable substructures in interaction

networks' (see [29] for references), but this definition is not operational according to our view because many distinct types of 'substructures' can be conceived. In the majority of papers, a module is considered to be composed of interacting species from both sets such that within-module interactions are more common than between-module relationships (e.g. [30]). Modules may be entirely separated from outside but completely connected within, and these extreme cases are often called 'compartments' [31]. However, distinction between the two terms is not always clear and some authors use the two terms interchangeably [32]. To avoid confusions, we shall use the term module only. Here, as the examples that follow will illustrate, 'ideal' modules manifest themselves as rectangular blocks filled entirely with 1's in the interaction matrix (complete connectance inside the module), such that the species included have no links outside the blocks. A bipartite graph is said to have perfectly modular structure if the interaction matrix contains ideal blocks only (as examples, see toy matrices d, e and f in Supplementary Appendix 1, Fig. A.1.1), a situation never appearing in nature. Figure 3 shows that whenever modules are not perfect but still considerably compact and fairly isolated from one another, the points are clustered into two groups within the simplex triangle: one at the R corner and the upper part of the I side, and the other at the similarity (S) corner. Thus, projection of points to the I-simplex shows bimodal distribution, a phenomenon long observed for the Jaccard similarity values between species in food webs [22]. Bimodality is strong when the blocks are equal in size (Fig. 3a), but differences between sizes of modules—and therefore differences in degree—force the upper group of points to move towards the D corner (Fig. 3b). Similar conclusions can be made if the matrices are examined by rows. Thus, to express bimodality of the distribution, and therefore modality in the matrix quantitatively, we suggest a novel measure WD (standing for 'weighted distance' between modes). It involves examination of this distribution for both the columns and the rows and is calculated as the weighted difference between the left and right modes of these distributions whenever the left peaks exist. Weights reflect the proportion of node pairs pertaining to the nodes: the higher this ratio is, the more expressed are the peaks in the distribution (see detailed description of the method in Supplementary Appendix 1).

Extreme or perfect modularity and complete nestedness are sometimes conceived as endpoints of an 'hypothetical' structural continuum of bipartite networks (cf. [12]). Because strict nestedness (N') takes minimum and maximum for these endpoints, respectively, we suggest the use of this function to refine the results obtained by the WD measure. The idea is that these two descriptors taken together reveal more information on the existence of modules than either one inspected alone. The relationships between WD and N' can be visualized in a two-dimensional scatter plot, with WD as the horizontal axis and strict nestedness as the vertical axis, and the points corresponding to bipartite networks. Supplementary Appendix 1 provides details and artificial examples showing that, at least for the artificial examples, nestedness and modularity are largely negatively related and that these two measures do not combine arbitrarily (Supplementary Appendix 1, Fig. A.1.1A). Our analysis described later will reveal whether this relationship holds true for real-world bipartite networks as well.

Notwithstanding negative correlation, a zero value for N' does not mean presence of modular structures automatically. Also, large weighted distance between modes is uninformative, for example, on the number of modules. As illustrated by Fig. A.1.1 in Supplementary Appendix 1, different but perfectly modular matrices can therefore take the same position in the WD-versus-nestedness plot. For recovering modular structures in interaction networks even more clearly, we propose a further tool, namely the use of the centroid scores on the I-simplex which separate overlapping modular matrices in another two-dimensional plot (Supplementary Appendix 1, Fig. A.1.1B).

To sum it up, we suggest that the existence of modular structural elements in bipartite graphs is indicated considerably well by using three different matrix descriptor variables simultaneously: the weighted distance between modes in the distribution of the Jaccard coefficient, and the means of strict

nestedness and interaction dissimilarity, all based on the pairwise comparison of species separately for both domains. Scatter diagrams show the interplay between these network characteristics and are useful to decide whether a given network is worth further analysing by more sophisticated algorithms of modularity detection.

4. Architectural asymmetry in bipartite networks

The fact that structure in interaction matrices is examined using the SDR simplex by selecting any of the two partner sets as the focal group, M or P, gives the opportunity to express architectural network (a)symmetry numerically. Symmetry is understood here in the general sense that the graph for one set of nodes is identical in some property to the partner set of the nodes and asymmetry is the departure from this identity. For example, web asymmetry is commonly—and extremely simply—quantified as the balance between the number of nodes in the two sets [11,14]. Here, we go a bit further by considering a bipartite network symmetric if the centroids in the two SDR plots coincide, while distant centroids are indicative of structural asymmetry. Thus, we suggest as a *simple measure of asymmetry* the use of Euclidean distance between the centroids, as given by the following formula:

$$\kappa = \sqrt{(\bar{S}_P - \bar{S}_M)^2 + (\bar{D}_P - \bar{D}_M)^2 + (\bar{R}_P - \bar{R}_M)^2}, \quad (5)$$

where \bar{S}_P refers to the mean interaction similarity for focal group P, and so on (Supplementary Appendix 1, equations A1.1 to A1.3). κ is zero if the centroids coincide, while the theoretical maximum is $\sqrt{2}$, never reached under realistic conditions ($\sqrt{2}$ is obtained for the lower left matrix in Fig. 2c). As an illustration, consider first the slightly perturbed modular structures in Fig. 3, which appear fairly symmetric at first sight. The fact that similar structure emerges regardless of whether the matrix is viewed by columns or rows is confirmed by the κ measure, which is 0.03 for matrix A and 0.08 for matrix B. The higher second value reflects size differences between modules. Agreement between visual inspection of the SDR simplex plot and the κ measure is further demonstrated by Fig. A.2.1 in the Supplementary Appendix 2 for random graphs. Actual examples are discussed in the next section.

5. Analysis of real-world bipartite ecological networks

5.1 Unweighted networks

The SDR simplex method is applied to a total of 172 unweighted bipartite networks published in the literature, taken from Internet resources or placed kindly at our disposal by colleagues (see Acknowledgements). The data set includes 77 host–parasite, 48 plant–pollinator, 5 plant–herbivore, 3 ant–plant, 31 plant–seed disperser, 2 anemone–fish and 6 plant–mycorrhiza networks. Here, we do not report all the results, but restrict our discussion briefly to those examples that exhibit extreme values for one or more SDR scores.

- The Illinois plant–pollinator network [33] is outstanding in the present study for several respects (Fig. 4a and b). It has the largest interaction matrix analysed (1044 pollinator species and 456 plants), with plants as the focal group link replacement is the highest ($R = 82.12\%$, Fig. 4a), while for the pollinators interaction dissimilarity is the maximum found in this study ($I = 99.003\%$, Fig. 4b). Network asymmetry is also very high ($\kappa = 0.55$) because degree difference is much less emphasized for the plants than for the pollinators (i.e. insects differ from one another much more in the number of plants they pollinate, than plants do in the number of their pollinators).

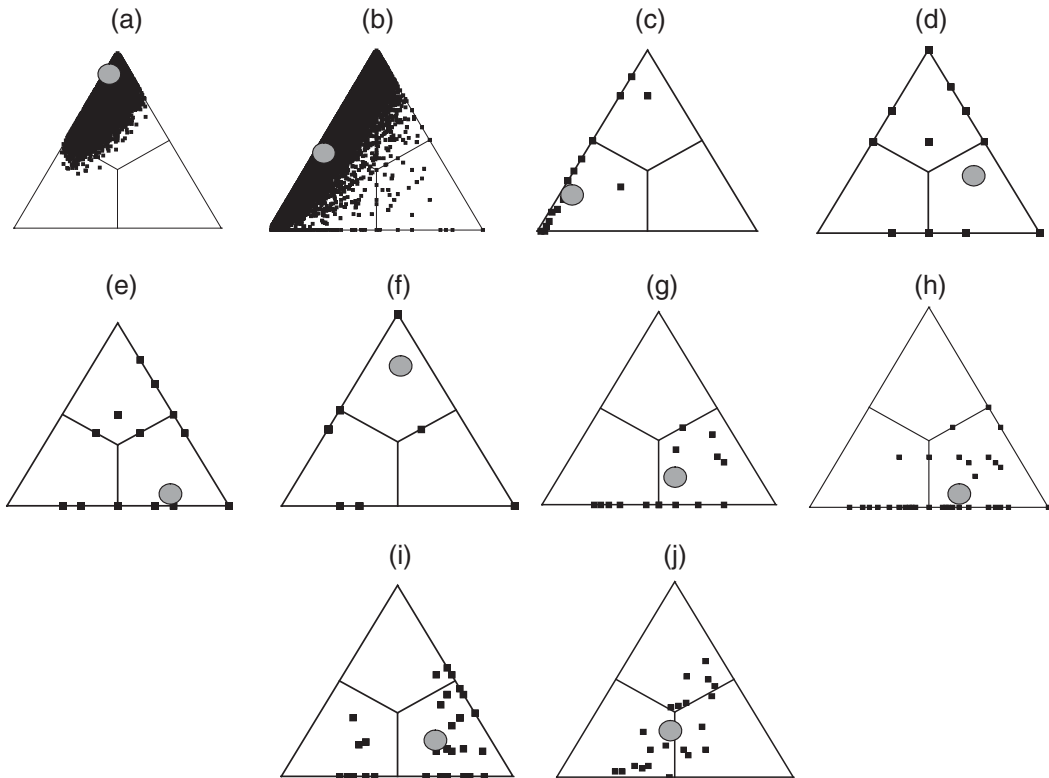


FIG. 4. The SDR simplex plot for some selected examples from the studied set of unweighted networks. Grey symbols indicate the centroid of point scatter within each triangle. (a) Illinois plants–pollinators network, plants [33]; (b) Illinois plants–pollinators network, pollinators [33]; (c) *Prunus* species–butterflies network from Britain, trees [34]; (d) *Prunus* species–butterflies network from Britain, butterflies [34]; (e) *Prunus* species–butterflies network from Finland, butterflies [34]; (f) plants–pollinators network in the Galapagos Islands, pollinators [35]; (g) ‘turnnog’ plants–seed dispersers network, plants [4]; (h) oil flowers–pollinators network, pollinators [36]; (i) plants–seed dispersers network by Frost, birds [37]; (j) plants–mycorrhiza network, trees [38].

- The *Prunus*–butterfly network from Britain (6 tree species, 88 butterflies, [34]) is remarkable for its high level of degree difference for the tree species ($D = 66.66\%$, Fig. 4c), showing that the plants differ strongly in the quality of food (nectar) they offer to insects. The butterflies nevertheless have a much more even degree distribution, causing this network to exhibit the highest architectural asymmetry among the networks studied ($\kappa = 0.67$, Fig. 4c and d).
- Interaction similarity is maximum, $S = 70.96\%$, for the insects in another *Prunus*–butterfly network from Finland ([34], see Fig. 4e) which is mainly responsible for its top value for nestedness as well ($N = 97.76\%$). This indicates relatively low nutrition specificity in a nested arrangement.
- Maximum degree agreement is $A = 89.34$, obtained for the pollinators in the Galapagos Islands ([35], Fig. 4f). This is because 20 of the 22 species pollinate only one species each—thus causing most points to fall exactly on the S or the R corner.
- Strict nestedness (i.e. when nodes with equal degree are ignored) is the highest ($N' = 89.86$) for the plants in the small plant–seed disperser network ‘turnnog’ (Jordano unpubl., cited in [4], Fig. 4g)

and is also remarkable ($N' = 86.7$, Fig. 4h) for the pollinators in the oil flowers example [36]. Connectance reaches the maximum for the birds as the focal group in the network described by Frost ([37], taken from [4]), for which nestedness is also exceedingly high (Fig. 4i).

- A more balanced situation also deserves our attention: for the deciduous forest trees in a plant–mycorrhiza network [38], similarity and degree difference contribute equally, while link replacement is only slightly lower. As a result, the point cloud is arranged along the A-simplex (Fig. 4j)—a common feature of balanced sites by species data matrices observed by Podani and Schmera [16].

Modularity is examined for all networks using the three descriptors WD%, N' % and I % (Fig. 5a). The overwhelming majority of networks are positioned on the lower right part of the plot, below WD = 100% and $N' = 100%$ and over $I = 100%$ (the latter one indicated on a grey scale), which shows that most of real-world networks do not exhibit high levels of modularity and strict nestedness, while the balance is turned over in favour of high dissimilarities. This means that modules, if exist, are small so that some interaction matrices are hardly distinguishable from sparse random matrices and diagonally structured ones.

- On bottom right of this plot, an arrow points to an Amazonian ant–plant network [39] which takes the rightmost position in the plot. After examining the structure of the interaction matrix (Fig. 5a, inset, network #119), we find many small modules, i.e. strong fragmentation, with remarkable similarity to toy matrices h and j . A small plant–pollinator network from the lava deserts of the Galapagos Islands [35] has similar structure (Fig. 5a, inset). Further three networks appear to exhibit modular structure (flea–mammal network from Nepal [40]; plant–pollinator network from the Andes, highest elevation [41]; and a flea–mammal network from Sugaty valley, Kazakhstan [42] cited in [43]). There are practically no networks exhibiting sharp modularity as suggested by some idealized textbook examples (e.g. Fig. 10.16 in [44]).
- The other arrow points to the position taken by the large Galapagos pollination network obtained for multiple communities [45]. Rearranged to optimal structure for either modularity or nestedness, we see that it has a more complex pattern and part of modularity comes from a few weakly modular units, while nestedness is due largely to a single generalist plant and a single generalist pollinator (Supplementary Appendix 2, Fig. A.2.4A and B).
- The topmost positions are taken by networks with high strict nestedness values (plant–bird network from Trinidad [46] and flea–mammal network from Korea [47]; Fig. 5a, insets), which, therefore, have no modular structure at all. Even though these matrices were rearranged to optimize diagonal ordering, nestedness is still apparent.
- Several very large matrices have neither nested nor modular structures; these are found on the lower left part of the diagram (e.g. Illinois plant–pollinator [33], plant–pollinator network from Venezuela [48], avian–lice network, (L. Rózsa, unpubl.), tropical orchid–mycorrhiza network [49], Plant–leaf miner network from South America [6]).

5.2 Weighted networks

Of the networks evaluated on the basis of unweighted links, 108 had weights as well, namely 76 host–parasite, 17 plant–pollinator, 11 plant–seed disperser, 3 plant–ant and 1 plant–herbivore. As we did for unweighted networks, we select some of the most striking examples for demonstration and discussion.

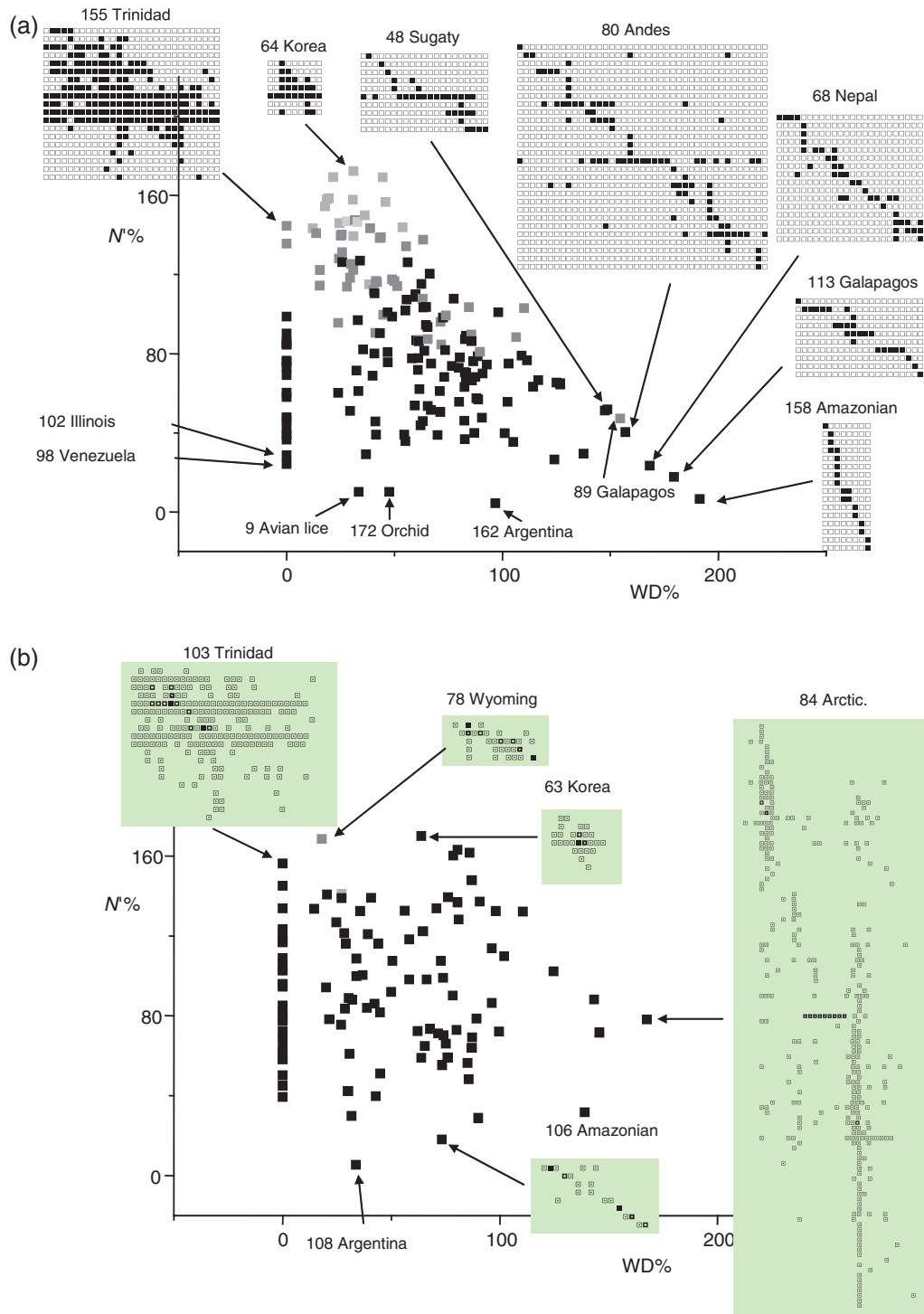


FIG. 5. Modularity plots for 172 unweighted (a) and 108 weighted (b) ecological bipartite networks using $WD\%$ as horizontal and $N\%$ as vertical axis. The third descriptor ($I\%$) is expressed on a grey scale applied to the symbols, from pale grey (lowest $I\%$) to black (highest $I\%$). Weighted links in the interaction matrices (insets in b) are represented by symbols \square , \square , \square and \blacksquare corresponding to four equal intervals in the range of the weights.

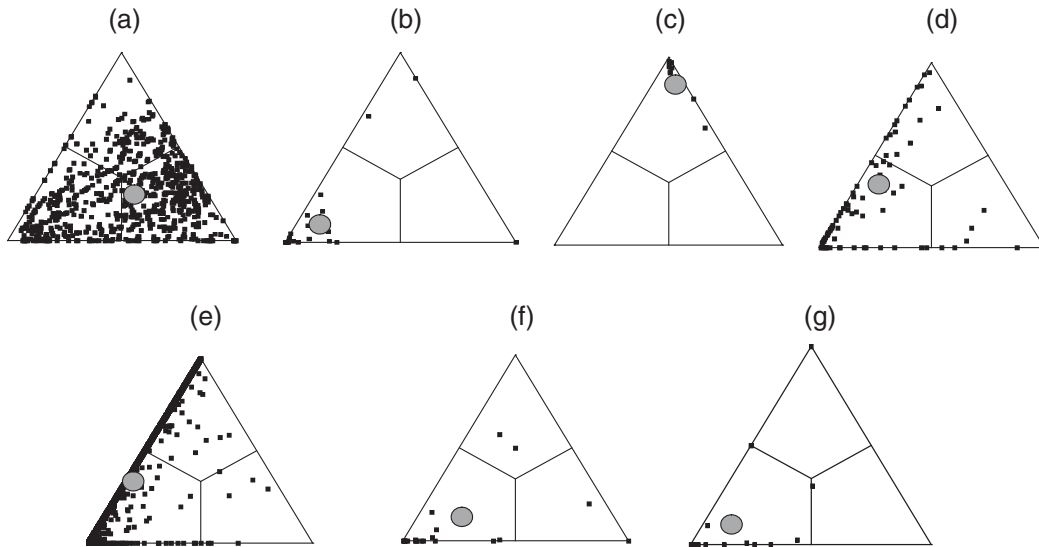


FIG. 6. The SDR simplex plot for some selected examples from the studied set of weighted networks. Grey symbols indicate the centroid of point scatter within each triangle. (a) Host–parasite part of the Carpentieria food web, hosts (max S) [50]; (b) Khasan, hosts (max D) [51]; (c) Wyoming, hosts (max R , A) [52]; (d) Wyoming, parasites [52]; (e) plant–leaf miner network South America, herbs [6]; (f) Korea, parasites (max N) [47]; (g) Korea hosts (max N') [47].

- Interaction similarity is the highest among the hosts in the host–parasite part of the Carpentieria salt marsh food web ($S = 40.5\%$, Fig. 6a [50]). That the maximum is only around 40 (compared with the maximum of 70 for the unweighted versions) reflects that weighting further increases differences between the species. In this particular case, it is nevertheless interesting that for the unweighted case similarity was only slightly higher ($S = 43\%$) than for the weighted case. A potential explanation is that the data are overwhelmed by low abundance values.
- Degree difference reached the maximum for the Khasan flea–mammal network, Russia, for hosts ($D = 83\%$, Fig. 6b; [51] cited in [43]).
- Link replacement and, at the same time, degree agreement have their maxima for hosts in the flea–mammal network from Wyoming ($R = 88\%$, $A = 98\%$, Fig. 6c; [52]) suggesting gradual shift of similar parasite abundances from one mammal species to the other. The Wyoming network has the highest architectural asymmetry as well ($\kappa = 0.892$) (compare Fig. 6c (hosts) and 6d (parasites)).
- Interaction dissimilarity was found to be the highest ($I = 99.7\%$, Fig. 6e) for the plants in the plant–herbivore network of Cagnolo et al. [6] reflecting an almost complete segregation of herbs with respect to herbivores.
- Nestedness is remarkably high for the parasites ($N = 89.9\%$) and strict nestedness is the highest for the hosts ($N' = 88.5\%$) in the same network, namely the flea–mammal network from Korea (Fig. 6f and g; [47]). The pattern of link replacement and degree agreement may be the outcome of some combination of carrying capacity and specialization. A certain amount of parasites is easily found, but too many of them would be dangerous for the host. Also, specialized parasites are probably successful in keeping potential new invaders away from the host.

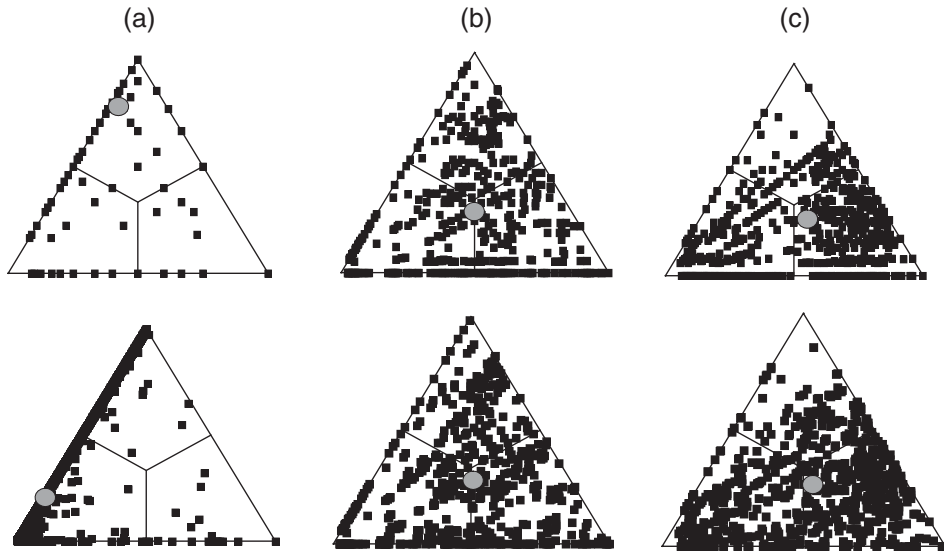


FIG. 7. The effect of weighting on network structure as reflected by the SDR simplex plot. Upper row: unweighted networks, lower row: weighted networks. (a) insects in the plant–leaf miner network, South America [6]; (b) parasites in the host–parasite part of the Carpentieria food web [50]; (c) hosts in the host–parasite part of the Carpentieria food web [50].

Weighting causes a more even distribution of networks in the modularity plot (Fig. 5b), while the $I\%$ values are almost always near the maximum (most symbols are dark grey or black).

- The strongest modular structure is detected for the arctic plant–pollinator network [53], explained by some clusters of extremely high weights. An ant–plant network [39] (strongest modularity in the unweighted case) has moved to the bottom centre, because the large weights form an obvious diagonal structure (see inset, Fig. 5b).
- Highest nestedness and lack of modularity were detected, for example, for two host–parasite networks (Korea, [47] and Wyoming, [52])—the first being in extreme position in the unweighted case as well—and the plant–pollinator network from Trinidad [46]. We call attention to another example, a plant–leaf miner network [6] which takes similar position in both networks.

5.3 The effect of weighting

Now, we compare weighted networks with their unweighted (binary) variants, so the sample from the real-world networks is the same as in the previous section. As a simple measure for the difference between weighted and unweighted versions of the same network, we use formula (5) modified as follows:

$$v = \sqrt{(\bar{S}_M - {}^w\bar{S}_M)^2 + (\bar{D}_M - {}^w\bar{D}_M)^2 + (\bar{R}_M - {}^w\bar{R}_M)^2} \quad (6)$$

for species set M . For the partner set P , the formula can be rewritten easily. Out of the 108 networks analysed, the largest difference was found for the herbivores in a plant–leaf miner network [6]. In this case, $v = 0.63$, while the SDR simplex diagrams are presented in Fig. 7a. Whereas interaction similarity is near zero in both cases, the unweighted version is dominated by link replacement. The move of

the centroid close to the D corner in the weighted network shows that emphasis is shifted towards excessive weight differences. The smallest difference between the centroids of the two versions of the same network, that is, the smallest effect of weighting, was detected for the host/parasite section of the *Carpenteria* food web [50]. v is only 0.02 for parasites and 0.03 for hosts, suggesting that the centroids for hosts and parasites almost coincide in the plot no matter if the network is weighted or not for both species sets (Fig. 7b and c). These observations support earlier studies reporting that weighting is more important in the case of food webs than for other network types [18].

6. Discussion

Bipartite networks representing mutualistic or antagonistic interactions between species have received increased attention in ecology in the past decades. Network structure has been most commonly assessed by emphasizing two features, nestedness and modularity, although some other graph theoretical descriptors are also considered in some reports (the topological importance index [54]; KeyPlayer analysis [13], or a suite of many network indices [14]). These studies largely underemphasized the importance of a common conceptual basis for linking the different measures. In this paper, we showed that the components contributing to the architectural diversity of bipartite ecological networks can be expressed by several pairwise functions pertaining to the same theoretical and methodological scheme. The formula behind our approach is Jaccard dissimilarity calculated between species pairs in either species domain, based on their relationships to the species of the other, and decomposed into additive fractions. Results may be expressed both graphically (ternary plots) and numerically (centroid scores and percentage contributions), a choice hardly available in other approaches. In the SDR simplex diagrams, points stand for species pairs, while tips and edges correspond to stand-alone and combined structural descriptors of the graph, respectively. The shape of the point cloud is useful to demonstrate whether certain features dominate within network structure (e.g. closeness of points to the nestedness side) or the entire network is heterogeneous (point cloud is spread all over within the plot). Since many points may overlap, especially if the number of species is large, it is also useful to show the position of the centroid of the point scatter. Centroid scores multiplied by 100 are conceived as percentage contributions of the basic features (S = interaction similarity, D = degree difference and R = link replacement) to overall network structure. Combining two of these at a time produce further measures, namely nestedness ($S + D$), interaction dissimilarity ($D + R$) or degree agreement ($S + R$).

As a further advantage, one has the opportunity to examine a given network based on unweighted or weighted links in a logically comparable manner. A fundamental property is order invariance: the results do not depend on the sequence by which rows and columns are presented in the matrix for analysis. Since the indices involved are all relativized, the size of networks poses no problems for the investigator, facilitating comparisons between networks and subsequent meta-analyses. These novelties together specify an efficient analytical toolkit for network science, allowing comparative studies of bipartite networks in the future.

The main achievement in this paper is the SDR simplex and its variant applicable to weighted networks. Indirectly, the method is linked to the detection of modularity as well, because the distribution of interaction dissimilarity values is useful in this regard. We can only confirm the general view that detecting modularity in bipartite networks is a complex matter, requiring sophisticated algorithms (such as simulated annealing), pre-defined run parameters (e.g. number of modules) and facing difficulties with large graphs [4,10,29,55,56]. Nevertheless, modularity of network architecture can be evaluated indirectly, rapidly and relatively easily by the simplex approach for any network size, as compared to other modularity algorithms which usually require much more computing time. Our conjecture is that

there is no single, one-valued function that can be used by itself to quantify the oft-mentioned contrast between nestedness and modularity for any interaction matrix. We have suggested that the modularity problem requires a three-dimensional approximation, using a coefficient of bimodality in the distribution of interaction dissimilarity, and measures of mean strict nestedness and mean interaction dissimilarity, calculated in a two-way mode on the interaction matrix. Candidates for modular matrices can be identified on the basis of low nestedness and high bimodality, and then insight into the number of modules is obtained by examining mean interaction dissimilarity. Portrayed for many ecological networks in a two-dimensional scatter plot, most unweighted networks are constrained to a relatively small portion of the state-space, reflecting that networks are dominated by extremely fragmented modules or gradient-like structures in all biological types (both antagonistic and mutualistic). This confirms the conclusions by Trøjelsgaard and Olesen [57] who found that 5 was the minimum number of modules in a set of 54 networks. This cannot be attributed only to the fact that connectance rarely exceeded 50% in the networks studied here, but also to the lack of bimodality in the distribution of I . This effect is even more pronounced for weighted links because strong interactions are relatively rare in the real world.

We must admit, however, that the weighted mode distance measure, mean strict nestedness and mean interaction dissimilarity and therefore positions in the modularity plot are useful to get only some first insights into potential compartmentalization, and cannot substitute more sophisticated module-seeking algorithms.

Asymmetry is a property of bipartite networks whose measurement is more straightforward via SDR-simplices than that of modularity. Recall that our approach can examine a network in two alternative ways: starting from dissimilarities between species of either domain, e.g. for hosts as well as for parasites. (Construction of the modularity plot mentioned in the previous paragraph was already based on this double view.) We propose the distance between the centroids in the two simplex plots as a simple measure of asymmetry of the bipartite graph, while acknowledge that this is only the first step towards defining more sophisticated coefficients of symmetry. Based on this, we conclude that the majority of real-world bipartite networks are reasonably symmetric (mean κ asymmetry ~ 0.1 – 0.15) regardless of weighting. In the near past, asymmetry was also measured with focus on a particular property of the graph, for example, as a balance between the number of species in the two sets [11]. For weighted networks, Bascompte *et al.* [3] measured asymmetry of interaction strength separately for each possible pair of related species, while Maeng and Lee [58] compared the distributions of interaction strength between plants and pollinators to devise an overall coefficient. It is obvious from these papers, as well as from [59] that the concept of asymmetry is equivocal, and differences in practically any measure of network structure calculated for the two sets of species can be considered as a rough indication of asymmetry. We plan, therefore, to expand our measure such that more information on the distribution of points within the triangle plots will be used to express structural asymmetry more faithfully.

As an introduction to new concepts and methods, we did not exhaust all the possibilities offered by the SDR simplex and associated tools. Our emphasis was placed on the explorative analysis of pattern in bipartite networks, so we did not examine possibilities of using different null models and statistical tests. Employing null models to test the significance of network properties would have made the present study overly complicated. We understand that significance testing based on various null models must be an essential part of any quantitative network study, and therefore plan to report on progress into this direction in a separate study.

Our study focused on ecological bipartite networks, while many artificial examples were provided to facilitate understanding of the new methodology. Thus, we expect with good reason that the simplex approach may be useful in other fields of science in which bipartite graphs have practical importance (see examples in [7]).

7. Supplementary data

Supplementary data are available at *Journal of Complex Networks* online.

Acknowledgement

We are extremely grateful to J. Bascompte, B. Krasnov, R. Poulin, L. Rózsa, and L. Cagnolo for generously making their network data available to us. We benefited much from discussions with P. Erdős and I. Miklós at Alfréd Rényi Institute of Mathematics. Our study would have been almost impossible to do without the free Internet resources offered by NCEAS (National Center for Ecological Analysis and Synthesis) at the University of California, Santa Barbara, USA.

Funding

The research was supported by the Hungarian Scientific Research Fund (OTKA K104279).

REFERENCES

- MEMMOTT, J. (1999) The structure of a plant-pollinator food web. *Ecol. Lett.*, **2**, 276–280.
- MÜLLER, C. B. & GODFRAY, H. C. J. (1999) Indirect interactions in aphid-parasitoid communities. *Res. Popul. Ecol.*, **41**, 93–106.
- BASCOMPTE, J., JORDANO, P. & OLESEN, J. M. (2006) Asymmetric coevolutionary networks facilitate biodiversity maintenance. *Science*, **312**, 431–433.
- FORTUNA, M. A., STOFFER, D. B., OLESEN, J. M., JORDANO, P., MOUILLOT, D., KRASNOV, B. R., POULIN, R. & BASCOMPTE, J. (2010) Nestedness versus modularity in ecological networks: two sides of the same coin? *J. Animal Ecol.*, **79**, 811–817.
- THÉBAULT, E. & FONTAINE, C. (2010) Stability of ecological communities and the architecture of mutualistic and trophic networks. *Science*, **329**, 853–856.
- CAGNOLO, L., SALVO, A. & VALLADARES, G. (2011) Network topology: patterns and mechanisms in plant-herbivore and host-parasitoid food webs. *J. Animal Ecol.*, **80**, 342–351.
- ASRATIAN, A. S., DENLEY, T. M. J. & HÄGGKVIST, R. (2008) *Bipartite Graphs and their Applications*. Cambridge: Cambridge University Press.
- JORDANO, P. (2013) Lab dataset. <http://ebd10.ebd.csic.es/ebd10/Datasets.html>. Accessed on 18 July 2013.
- NCEAS (2013). Interaction Web DataBase. www.nceas.ucsb.edu/interactionweb/. Accessed on 17 July 2013.
- OLESEN, J. M., BASCOMPTE, J., DUPONT, Y. L. & JORDANO, P. (2007) The modularity of pollination networks. *Proc. Natl Acad. Sci. USA*, **104**, 19891–19896.
- BLÜTHGEN, N., MENZEL, F., HOVESTADT, T., FIALA, B. & BLÜTHGEN, N. (2007) Specialization, constraints and conflicting interests in mutualistic networks. *Curr. Biol.*, **17**, 1–6.
- LEWINSOHN, T. M., PRADO, P. I., JORDANO, P., BASCOMPTE, J. & OLESEN, J. M. (2006) Structure in plant-animal interaction assemblages. *Oikos*, **113**, 174–184.
- BENEDEK, Z., JORDÁN, F. & BÁLDI, A. (2007) Topological keystone species complexes in ecological interaction networks. *Community Ecol.*, **8**, 1–8.
- DORMANN, C. F., BLÜTHGEN, J., FRÜND, N. & GRUBER, B. (2009) Indices, graphs and null models: analyzing bipartite ecological networks. *Open Ecol. J.*, **2**, 7–24.
- VACHER, C., PIOUS, D. & DESPREZ-LOUSTAU, M.-L. (2008) Architecture of an antagonistic tree/fungus network: the asymmetric influence of past evolutionary history. *PLoS ONE*, **3**, e1740.
- PODANI, J. & SCHMERA, D. (2011) A new conceptual and methodological framework for exploring and explaining pattern in presence-absence data. *Oikos*, **120**, 1625–1638.

17. PODANI, J., RICOTTA, C. & SCHMERA, D. (2013) A general framework for analyzing beta diversity, nestedness and related community-level phenomena based on abundance data. *Ecol. Complex.*, **15**, 52–61.
18. SCOTTI, M., PODANI, J. & JORDÁN, F. (2007) Weighting, scale dependence and indirect effects in ecological networks: a comparative study. *Ecol. Complex.*, **4**, 148–159.
19. JACCARD, P. (1901) Distribution de la flore alpine dans le bassin des Dranses et dans quelques régions voisines. *Bulletin de la Société Vaudoise des Sciences Naturelles*, **37**, 241–272.
20. SUGIHARA, G., SCHOENLY, K. & TROMBLA, A. (1989) Scale invariance in food web properties. *Science*, **245**, 48–52.
21. MARTINEZ, N. D. (1991) Artifacts or attributes? Effects of resolution on the Little Rock Lake food web. *Ecol. Monogr.*, **61**, 367–392.
22. RAFFAELLI, D. & HALL, S. J. (1992) Compartments and predation in an estuarine food web. *J. Animal Ecol.*, **61**, 551–560.
23. YODZIS, P. & WINEMILLER, K. O. (1999) In search of operational trophospecies in a tropical aquatic food web. *Oikos*, **87**, 327–340.
24. KLEIN, A. M., MÜLLER, C., HOEHN, P. & KREMEN, C. (2009) Understanding the role of species richness for crop pollination services. *Biodiversity, Ecosystem Functioning, and Human Wellbeing—An Ecological and Economic Perspective* (S. Naeem, D. E. Bunker, A. Hector, M. Loreau & C. Perrings eds). Oxford: Oxford University Press, pp. 195–208.
25. CARVALHO, J. C., CARDOSO, P. & GOMES, P. (2012). Determining the relative roles of species replacement and species richness differences in generating beta-diversity patterns. *Global Ecol. Biogeogr.*, **21**, 760–771.
26. BASCOMPTE, J., JORDANO, P., MELIÁN, C. J. & OLESEN, J. M. (2003) The nested assembly of plant–animal mutualistic networks. *PNAS*, **100**, 9383–9387.
27. PODANI, J. & SCHMERA, D. (2012) A comparative evaluation of pairwise nestedness measures. *Ecography*, **35**, 889–900.
28. ULRICH, W. & ALMEIDA-NETO, M. (2012) On the meanings of nestedness: back to the basics. *Ecography*, **35**, 865–871.
29. DORMANN, C. F. & STRAUSS, R. (2013) Detecting modules in quantitative bipartite networks: the QuaBiMo algorithm. arxiv.org/pdf/1304.3218v.
30. NEWMAN, M. E. J. (2003) The structure and function of complex networks. *SIAM Rev.*, **45**, 167–256.
31. PIMM, S. L. (1982) *Food Webs*. Chicago: Chicago University Press.
32. THÉBAULT, E. (2012) Identifying compartments in presence-absence matrices and bipartite networks: insights into modularity measures. *J. Biogeogr.*, **40**, 759–768.
33. ROBERTSON, C. (1929) *Flowers and Insects: Lists of Visitors to Four Hundred and Fifty-Three Flowers*. Lancaster, PA, USA: Science Press Printing Company.
34. LEATHER, S. R. (1991) Feeding specialisation and host distribution of British and Finnish *Prunus* feeding macrolepidoptera. *Oikos*, **60**, 40–48.
35. PHILIPP, M., BÖCHER, J., STEGISMUND, H. R. & NIELSEN, L. R. (2006) Structure of a plant-pollinator network on a pahoehoe lava desert of the Galápagos Islands. *Ecography*, **29**, 531–540.
36. BEZERRA, E. L. S., MACHADO, I. C. & MELLO, M. A. R. (2009) Pollination networks of oil-flowers: a tiny world within the smallest of all worlds. *J. Animal Ecol.*, **78**, 1096–1101.
37. FROST, P. G. H. (1980) Fruit-frugivore interactions in a South African coastal dune forest. *Proc. Int. Ornitholog. Congr.*, **17**, 1179–1184.
38. FODOR, E. (2013) Linking biodiversity to mutualistic networks—woody species and ectomycorrhizal fungi. *Ann. Forest Res.*, **56**, 53–78.
39. DAVIDSON, D. W., SNELLING, R. R. & LONGINO, J. T. (1989) Competition among ants for myrmecophytes and the significance of plant trichomes. *Biotropica*, **21**, 64–73.
40. SMIT, F. G. A. M. (1974) Siphonaptera collected by Dr. J. Martens in Nepal. *Senckenbergiana Biol.*, **55**, 357–398.

41. ARROYO, M. T. K., PRIMACK, R. B. & ARMESTO, J. J. (1982) Community studies in pollination ecology in the high temperate Andes of Central Chile. I. Pollination mechanisms and altitudinal variation. *Amer. J. Bot.*, **69**, 82–97.
42. SABILAEV, A. S., DAVIDOVA, V. M. & POLE, D. S. (2003) About rodents' flea fauna on the left bank of the Ili river. *Quarantinable and Zoonotic Infections in Kazakhstan*, **7**, 148–149, in Russian.
43. KRASNOV, B. R., MOUILLOT, D., KHOKHLOVA, I., SHENBROT, G. I. & POULIN, R. (2008) Scale-invariance of niche breadth in fleas parasitic on small mammals. *Ecography*, **31**, 631–636.
44. MITTELBACH, G. G. (2012) *Community Ecology*. Sunderland: Sinauer.
45. MCMULLEN, C. K. (1993) Flower-visiting insects of the Galapagos Islands. *Pan-Pacific Entomol.*, **69**, 95–106.
46. SNOW, B. K. & SNOW, D. W. (1988) *Birds and Berries: A Study of an Ecological Interaction*. London: Poyser.
47. WALTON, D. W. & HONG, H. K. (1976) Fleas of small mammals from the endemic haemorrhagic fever zones of Kyonggi and Hangwon provinces of the Republic of Korea. *Korean J. Parasitol.*, **14**, 17–24.
48. RAMIREZ, N. & BRITO, Y. (1992) Pollination biology in a Palm Swamp Community in the Venezuelan Central Plains. *Bot. J. Linnean Soc.*, **110**, 277–302.
49. MARTOS, F., MUNOZ, F., PAILLER, T., KOTTKE, I., GONNEAU, C. & SELOSSE, M. A. (2012) The role of epiphytism in architecture and evolutionary constraint within mycorrhizal networks of tropical orchids. *Mol. Ecol.*, **20**, 5098–5109.
50. LAFFERTY, K. D., HECHINGER, R. F., SHAW, J. C., WHITNEY, K. L. & KURIS, A. M. (2006) Food webs and parasites in a salt marsh ecosystem. *Disease Ecology: Community Structure and Pathogen Dynamics* (S. Collinge & C. Ray eds). Oxford: Oxford University Press, pp. 119–134.
51. LEONOV, Y. A. (1958) Fleas parasitic on rodents of the southern part of Primorye (Far East). *Proc. of Irkutsk State Scientific Anti-Plague Institute Siberia Far East*, **17**, 147–152 (in Russian).
52. ANDERSON, S. H. & WILLIAMS, E. S. (1997) Plague in a complex of white-tailed prairie dogs and associated small mammals in Wyoming. *J. Wildlife Dis.*, **33**, 720–732.
53. KEVAN, P. G. (1970) High arctic insect-flower visitor relations: the inter-relationships of arthropods and flowers at Lake Hazen, Ellesmere Island, Northwest Territories, Canada. *PhD thesis*, University of Alberta.
54. JORDÁN, F., LIU, W.-C. & VAN VEEN, F. (2003) Quantifying the importance of species and their interactions in a host-parasitoid community. *Community Ecol.*, **4**, 79–88.
55. NEWMAN, M. E. J. & GIRVAN, M. (2004) Finding and evaluating community structure in networks. *Phys. Rev. E*, **69**, 026113.
56. GUIMERÀ, R. & AMARAL, L. A. N. (2005) Functional cartography of complex metabolic networks. *Nature*, **433**, 895–900.
57. TRØJELSGAARD, K. & OLESEN, J. M. (2013) Macroecology of pollination networks. *Global Ecol. Biogeogr.*, **22**, 149–162.
58. MAENG, S. E. & LEE, J. W. (2011) Asymmetric network properties of bipartite ecological networks. *J. Korean Phys. Soc.*, **58**, 851–854.
59. CRUZ, P. T., DE ALMEIDA, A. M. & CORSO, G. (2011) Measuring asymmetry in insect-plant networks. *J. Phys.: Conf. Ser.*, **285**, 012029.